European Coordination for Accelerator Research and Development

PUBLICATION

Operation of the superconducting RF photo gun at ELBE

Teichert, J (HZDR) *et al*

02 April 2012

The research leading to these results has received funding from the European Commission under the FP7 Research Infrastructures project EuCARD, grant agreement no. 227579.

This work is part of EuCARD Work Package **10: SC RF technology for higher intensity proton accelerators and higher energy electron linacs**.

The electronic version of this EuCARD Publication is available via the EuCARD web site <http://cern.ch/eucard> or on the CERN Document Server at the following URL : <http://cdsweb.cern.ch/record/1436382

Operation of the superconducting RF photo gun at ELBE

2011 J. Phys.: Conf. Ser. 298 012008

(http://iopscience.iop.org/1742-6596/298/1/012008)

Journal of Physics: Conference Series **298** (2011) 012008 doi:10.1088/1742-6596/298/1/012008

Operation of the superconducting RF photo gun at ELBE

J Teichert[1,5], A Arnold[1], H Büttig[1], U Lehnert[1], P Michel[1], P Murcek[1], Ch Schneider[1], R Schurig[1], G Staats[1], R Xiang[1], P Kneisel[2], T Kamps[3], J. Rudolph[3], M. Schenk[3], G. Klemz[4] and I Will[4]

[1] Forschungszentrum Dresden-Rossendorf, P O Box 510119, 01314 Dresden, Germany
[2] Thomas Jefferson National Accelerator Facility, 12000 Jefferson Avenue, Newport News, VA 23606, USA
[3] Helmholtz-Zentrum Berlin, Albert-Einstein-Str. 15, 12489 Berlin, Germany
[4] Max-Born-Institut, Max-Born-Str. 2, 12489 Berlin, Germany

E-mail: j.teichert@fzd.de

Abstract. As the first superconducting RF photo-injector (SRF gun) in practical operation, the SRF gun has been successfully connected to the superconducting linac ELBE at Forschungzentrum Dresden-Rossendorf. The injection with this new gun will improve the beam quality for the users of the radiation source. The SRF gun contains a 3½ cell superconducting accelerating cavity with a frequency of 1.3 GHz. The design is for use of normal conducting photocathodes. At present, caesium telluride photocathodes are applied which are illuminated by an ultraviolet laser beam. The kinetic energy of the produced electron beam is 3 MeV which belongs to a peak electric field of 16 MV/m in the cavity. The maximum bunch charge which is obtained and measured in a Faraday cup is about 400 pC (20 μA average current at a repetition rate of 50 kHz). The SRF gun injector is connected to the ELBE accelerator via a dogleg with two 45° deflection magnets. This connection beam line was commissioned in January 2010. A first beam injection into the ELBE accelerator has been carried out with a bunch charge of 120 pC (6 μA at 50 kHz). Detailed measurements showed that beam loss occurred in the dogleg above 60 pC due to the correlated energy spread. In order to find the optimal operation conditions, energy spread was measured in dependence of bunch charge, laser phase and further gun parameters. The Cs_2Te photocathode shows an excellent life time. It is in the gun since May 2010 with about 300 h beam time and about 7 C extracted charge. In the present cavity, the limit for the acceleration gradient is field emission due to some defect on the cavity surface and problems during cleaning. Therefore a modified 3½ niobium cavity has been fabricated, which will increase the RF gradient in the gun and thus improve the beam parameters further.

1. Introduction

Future accelerator based radiation sources need high-brightness electron beams with high average currents and pulse repetition rates in the megahertz rage. Electron guns which can provide beams with these properties are still under development. The most promising candidate is the superconducting photo electron injector (SRF gun). The basics operation principle of a SRF gun is the direct production

[5] To whom any correspondence should be addressed

of short electron pulses by laser irradiation of a photocathode which is placed in a RF resonator. The RF field ensures an instantaneous and strong acceleration of the electron bunches. The superconducting RF resonator has an extremely high quality factor and thus very low thermal losses which allows for a continuous wave (CW) operation. Compared to other CW guns, e.g. thermionic or DC voltage guns, the SRF gun has the highest gradient and acceleration voltages combination. Due to the low RF power losses, nearly all of the RF power is consumed for beam acceleration. And the SRF gun vacuum is ideal with an enormous cryopumping speed to provide best lifetime for sensitive photocathodes. At FZD a SRF gun was developed and commissioned [1] for the ELBE electron accelerator [2]. This gun is installed in the ELBE accelerator hall together with a sophisticated diagnostic beam line [3] and an UV driver laser system [4]. Until end of 2009 the SRF gun had solely been operated simultaneously to the ELBE user operation. The gun was optimized and the diagnostics commissioned. Measurements were carried out with respect to cryogenics, RF properties, photocathodes, and beam parameters and are published elsewhere [5]. During the 2009/2010 winter shutdown, the beam line was installed which connects the SRF gun to the ELBE linac.

2. Photocathodes

2.1. Preparation and exchange

The SRF gun requires photocathodes with quantum efficiency (QE) of 1 % or higher with a stability over weeks. The Cs_2Te photocathodes are chosen as the standard photocathodes. They are prepared in a special cathode lab and then transported to the accelerator hall. The tip of the cathode consists of molybdenum with 99.9 % purity and has 10 mm diameter. The Cs_2Te layer deposited on the top surface has 8 mm diameter. The deposition is done in vacuum between 10^{-9} and 10^{-8} mbar [6]. The QE of fresh photocathodes is between 8 % and 15 %. The cathodes are stored and transported to the SRF gun in a chamber with the vacuum of 2×10^{-10} - 1×10^{-9} mbar. The process of cathode transfer and also the operation in the SRF gun causes a quick decrease of the QE to about 1 %. On this level the QE remains stable and it seems that the photocathodes can serve for months in the SRF gun. A photocathode exchange needs about 30 min taking a fresh cathode from the storage chamber flanged to the gun. The exchange does not need a warm-up of the gun. The transport of the storage chamber from the cathode lab to the SRF gun and its docking at the load-lock needs one maintenance shift and a following one-week bake-out during accelerator operation.

2.2. Quantum efficiency and life time

Up to now five Cs_2Te photocathodes have been employed in the SRF gun. An overview is given in table 1. The first cathodes had poor quality due to insufficient vacuum or they were destroyed by accidentally venting during accelerator shut-downs. The present photocathode #250310Mo has served in the gun since four months with an accumulated beam time of about 300 h and a delivered charge of 6.4 C.

Table 1. Overview of Cs_2Te photocathodes used in the SRF gun.

Cathode no	Serving time	QE in gun	Delivered charge	Beam time
#090508Mo	23/5/08-23/6/08	0.05 %		
#070708Mo	21/7/08-19/9/08	0.1 %		
#310309Mo	08/5/09-24/8/09	1.1 %	0.8 C	~150 h
#040809Mo	24/8/09-23/3/10	0.6 %	0.7 C	~100 h
#250310Mo	25/5/10- in use	0.8 %	6.4 C	296 h

2.3. Thermal emittance

The term “thermal emittance” means the normalized transverse emittance of the electrons when they escape from the cathode surface. In the former thermionic guns, the thermal emittance is determined by the cathode temperature. However, for the semiconductor photocathodes the thermal emittance

depends on the energy excess, the electrons possess after absorption of a photon and emission. The normalized initial transverse emittance of a RF gun can be expressed as $\varepsilon_{n,rms}^2 \approx \varepsilon_{therm}^2 + \varepsilon_{sp}^2 + \varepsilon_{rf}^2$ and contains contributions of the thermal emittance ε_{therm}, the space charge part ε_{sp}, and the RF part ε_{rf}. In order to keep the second and third term small, the measurement of the transverse emittance must be carried out at very low bunch charge as well as the RF field should be low and the laser pulse short enough. These conditions are fulfilled in our experiments. A theoretical calculation of the thermal emittance for Cs_2Te cathode has been performed by Floettmann [7] within the three-step model with the result

$$\varepsilon_{therm} = \frac{x_{rms}}{\sqrt{3}} \sqrt{\frac{2E_{kin}}{m_0 c^2}} \quad . \tag{1}$$

In the formula x_{rms} is the rms laser spot size on the photocathode and E_{kin} is the electron kinetic energy given by $E_{kin} = E_{photon} - E_G - E_A$ with the photon energy E_{photon}, the band gap E_G, and the electron affinity E_A. By variation of the laser spot size, E_{kin} can be determined experimentally:

$$E_{kin} = \frac{3}{2} m_0 c^2 \left(\frac{d\varepsilon_{therm}}{dx_{rms}} \right)^2 \quad . \tag{2}$$

The wave length of the UV laser is 262nm, corresponding to the photon energy of 4.72 eV. The Cs_2Te semiconductor at liquid nitrogen temperature has the same band structure as the one at room temperature. According to Powell's measurement [8], the electrons will be excited to the final state in the conduction band with 4.05 eV above the valence band maximum. The band gap is 3.3eV, and the electron affinity is 0.2 eV for a fresh Cs_2Te photocathode film without external electric field. In such case, the electron kinetic energy can be calculated as E_{kin}= (4.05-3.3-0.2) eV = 0.55 eV. But for a polluted emission surface the electron affinity will be changed. Normally the absorption of rest gas will increase the electron affinity, which results in the degradation of QE.
The transverse emittance was measured versus rms laser spot size for different photocathodes with the results shown in figures 1and 2. The laser spot size was adjusted by changing the aperture diameter. The transverse emittance was determined by means of the solenoid scan method using the emittance compensation solenoid and the second YAG screen in the diagnostic beam line.

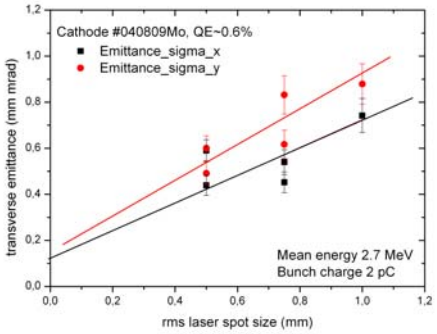

Figure 1. Emittance measurement versus laser spot size for cathode #040809Mo with QE = 0.6%.

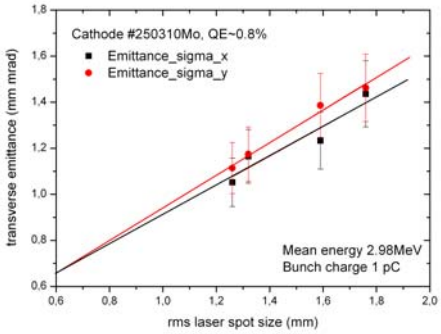

Figure 2. Emittance measurement versus laser spot size for cathode # 250310Mo with QE = 0.8%.

For cathode #040809Mo in figure 1, the slope of $\varepsilon_{rms,x}$ is 0.6 mrad, that of $\varepsilon_{rms,y}$ is 0.78 mrad. From equation 2, the average kinetic energy of the emitted photoelectrons E_{kin} was calculated to (0.38±0.1) eV, which means that the electron affinity is E_A= (0.37±0.1) eV. For cathode #250310Mo in

figure 2, the slope of $\varepsilon_{rms,x}$ is 0.64 mrad, that of $\varepsilon_{rms,y}$ is 0.71 mrad. The average kinetic energy E_{kin} was (0.35±0.04) eV, the electron affinity is E_A= (0.40±0.04) eV, about 0.2eV higher than that of the fresh cathode.

2.4. Multipacting

Multipacting is a well-known phenomenon frequently observed in RF systems and may cause serious problems. An analysis of the cavity, choke filter cell, and the other RF components during the design stage of the SRF gun showed a risk for multipacting in the opening where the cathode reach into the half-cell of the cavity. The RF field across the circular gap can accelerate electrons from one surface toward the other. Upon impact further electrons can be released. If the secondary emission coefficient is high enough and the field is resonant this process can continue and lead to multipacting. For that reason the photocathode can be biased with a high voltage to destroy the resonant condition. In fact, we observe this phenomenon during ramping up the RF field in the cavity and need up to 7 kV at the cathode to suppress it.

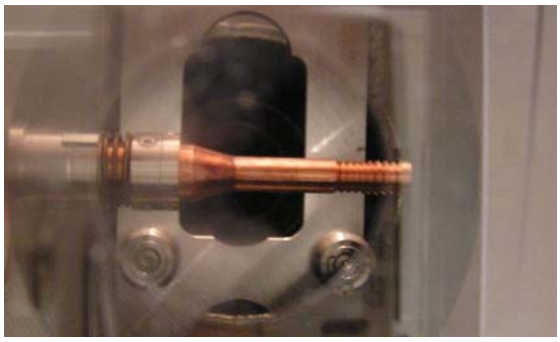

Figure 3. Modified photocathode stem with grooves for multipacting suppression.

Since the voltage needed varies more or less randomly, we looked for a method to prevent multipacting by another way. At BNL it was tried to suppress multipacting in the quarter wave choke filter by grooves [9] and a detailed study of multipacting suppression by fine grooving of a coaxial input coupler is presented in Ref [10]. In a similar way grooves has been machined in a cathode stem as it is shown in figure 3. In the critical region the cathode has wavelike grooves with 1 mm radius.

The success of the modified cathode geometry is presented in the time diagrams in figures 4. The curve in figure 4a shows the RF curve (gradient versus time) of a standard photocathode. The spikes indicate the appearance of cathode current due to multipacting. After some time the RF was turned off and then the ramp was started again with a higher DC voltage at the cathode. The curve in figure 4b shows the measurement for the grooved cathode. Here the multipacting is completely suppressed. Spikes occur neither for the slow RF ramp nor the following fast ramp.

3. SRF Gun Cavity and Beam Parameters

The quality degradation of the superconducting cavity due to pollution from the normal conducting photocathode in a SRF gun is still a question in discussion. For that reason the cavity performance has been measured regularly. The standard method is to determine the He consumption as function of the cavity gradient. From these data the unloaded quality factor can be calculated as it is shown in figure 5. The cavity can be operated until a peak field of 16 MV/m which corresponds to 6 MV/m acceleration gradient. After more than 650 h beam time, there is still no change in the cavity performance. After each shut-down with a cryomodule warm-up, the cavity was slightly worse. But a short high-power RF processing (HPP) reproduces the old values.

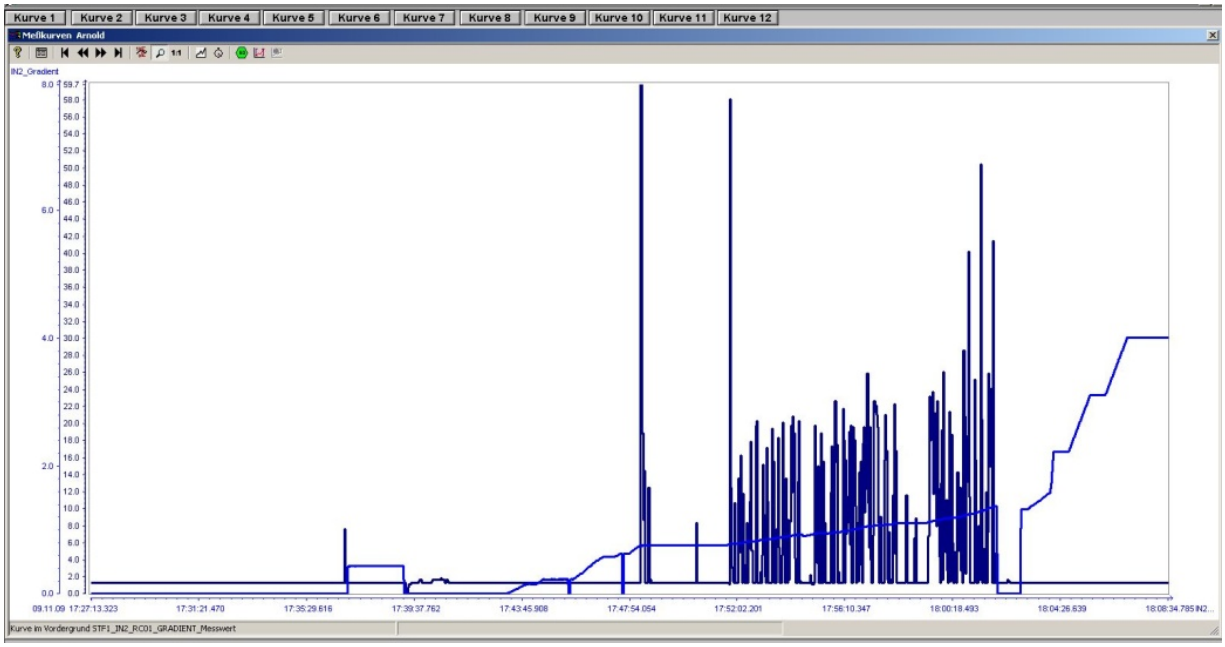

Figure 4a. Cavity gradient versus time during ramp-up for a standard photo cathode stem design. The spikes in the curve are multipacting events.

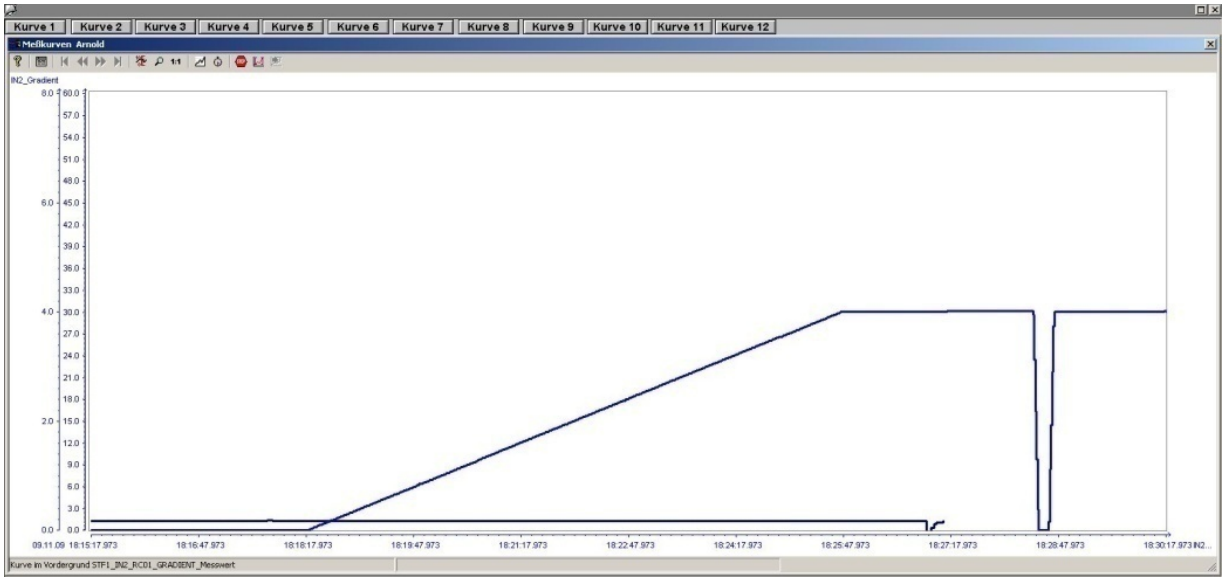

Figure 4b. Cavity gradient versus time during ramp-up for a grooved cathode stem. The curve does not show any multipacting events.

The SRF gun was operated with an acceleration gradient of 6 MV/m always in CW mode. Additionally a DC voltage of -5 kV was applied to the photocathode which slightly improves the beam parameters. The 263 nm laser beam was delivered by a Nd:YLF laser system with a 26 MHz oscillator, a regenerative amplifier, and frequency quadrupling. The average output power maximum was about 300 mW. The pulse repetition rate was chosen to 125 kHz (variable between 1 kHz and 250 kHz). The laser pulse is Gaussian in time with about 15 ps FWHM and had a nearly Gaussian lateral profile with 3.5 mm FWHM. The final kinetic energy and energy spread versus laser phase measured in the diagnostic beam line are presented in figures 6 and 7, respectively. For the SRF gun it is typical, that the electron energy has a broad maximum at low laser injection phases. The energy spread, mainly

correlated energy spread, is small for low laser phases and increases with higher laser phases and higher bunch charges. Since a low energy spread is important for the transmission in the dogleg, a low laser phase of 10° was used in the experiments.

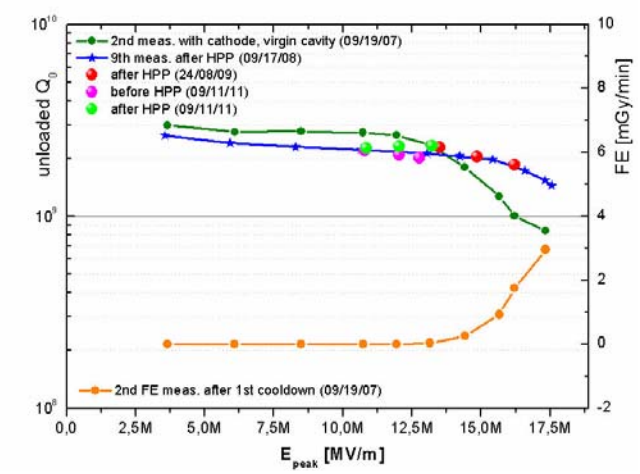

Figure 5. Performance of the SRF gun cavity. The diagram shows the unloaded quality factor versus RF peak field for several measurements and the corresponding field emission (FE).

The SRF gun was operated with an acceleration gradient of 6 MV/m always in CW mode. Additionally a DC voltage of -5 kV was applied to the photocathode which slightly improves the beam parameters. The 263 nm laser beam was delivered by a Nd:YLF laser system with a 26 MHz oscillator, a regenerative amplifier, and frequency quadrupling. The average output power maximum was about 300 mW. The pulse repetition rate was chosen to 125 kHz (variable between 1 kHz and 250 kHz). The laser pulse is Gaussian in time with about 15 ps FWHM and had a nearly Gaussian lateral profile with 3.5 mm FWHM. The final kinetic energy and energy spread versus laser phase measured in the diagnostic beam line are presented in figures 6 and 7, respectively. For the SRF gun it is typical, that the electron energy has a broad maximum at low laser injection phases. The energy spread, mainly correlated energy spread, is small for low laser phases and increases with higher laser phases and higher bunch charges. Since a low energy spread is important for the transmission in the dogleg, a low laser phase of 10° was used in the experiments.

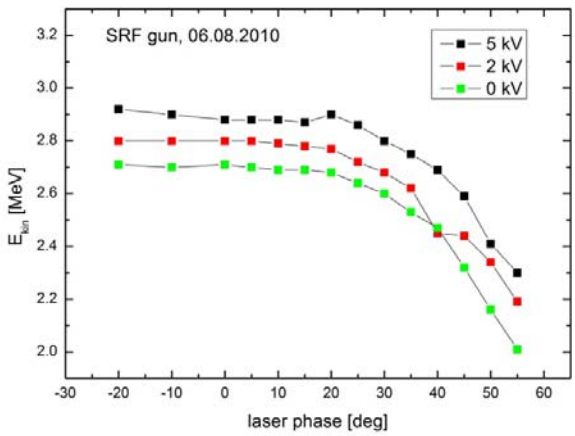

Figure 6. Measurement of the kinetic energy as function of laser phase for an acceleration gradient of 6 MV/m and different DC bias at the cathode.

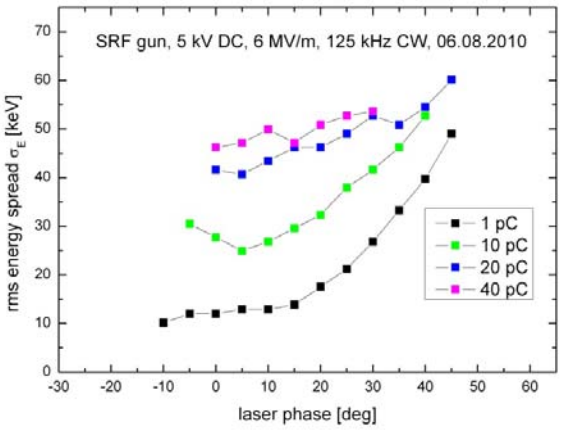

Figure 7. Energy spread at the SRF gun as function of laser phase for different bunch charges at an acceleration gradient of 6 MV/m and -5 kV cathode bias.

4. Beam for ELBE Linac

The beam line layout of SRF gun and ELBE linac is presented in figure 8. The beam line (dogleg), recently installed, connects the SRF gun injector with the ELBE linac. Usually ELBE is operated with the thermionic injector. Downstream the SRF gun a solenoid for emittance compensation is placed followed by a screen station, a movable Faraday cup for current measurements, and a quadrupole triplet. The new beam line starts about 1.5 m from the SRF gun exit with a 45° dipole magnet, which deflects the beam towards the ELBE linac, followed by a quadrupole triplet and ends with a second 45° magnet in front of the first acceleration module of ELBE.

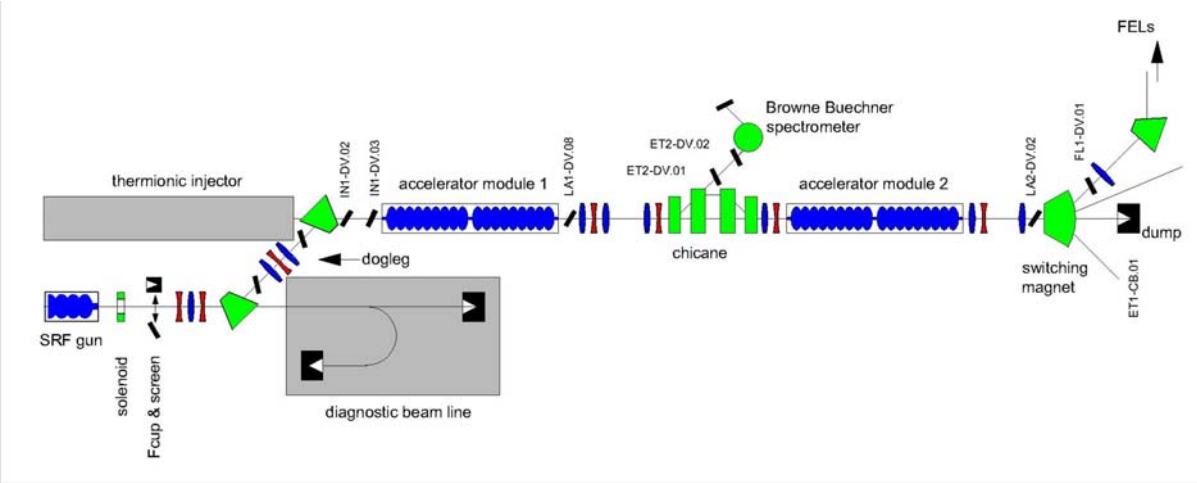

Figure 8. beam line layout of the SRF gun, dogleg section, and ELBE main accelerator.

The injection into the ELBE linac was carried out step by step, increasing the bunch charge. At low bunch charges the quadrupole triplet in the dogleg was adjusted towards an achromatic beam transport and maximum acceptance. After that, the on-crest phases of the first acceleration module were determined searching for maximum energy using the first chicane dipole. The first cavity was used to compensate the correlated energy spread of the gun, as it is shown in figure 9. The on-crest phase (maximum energy) in this measurement was found to be at 28°. The lowest energy spread turned out to be about -10° away. Finally the on-crest phases of the cavities of the second module were determined by means of energy measurement after the switching magnet.

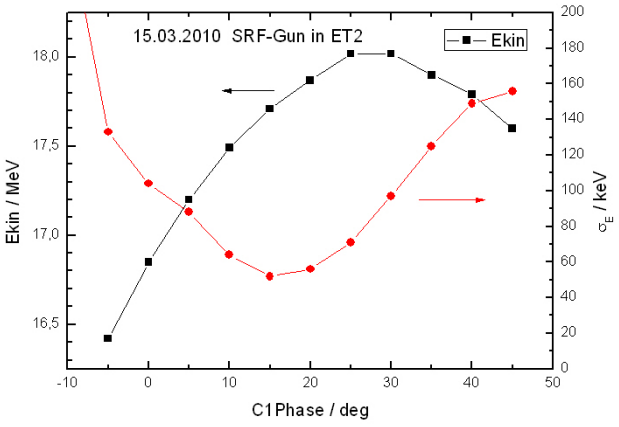

Figure 9. Measurement of energy and rms energy spread after the acceleration module 1 using the first dipole magnet of the chicane and YAG screen ET2-DV.01. The phase of the first cavity C1 was varied and the second cavity phase was held on crest.

Unfortunately, the large correlated energy spread of the SRF gun can be compensated only in the first cavity. Therefore the beam transport through the dogleg section is difficult. In a first test, a beam with

120 pC (6 µA at 50 kHz) was delivered to ELBE. The result of a second injection test is presented in figure 10. The transmission was obtained by comparing the beam currents measured in the Faraday cup near the SRF gun and in the beam dump downstream the switching magnet. Another indicator was the beam-loss monitoring system. The results of the current measurements are presented in figure 10. Up to 7.5 µA beam current (60 pC) the transmission was measured to be equal to one within measurement accuracy and no beam loss was monitored. For higher currents we found a strongly increasing beam loss in the dogleg section, which needs further optimization of the beam transport and gun parameters.

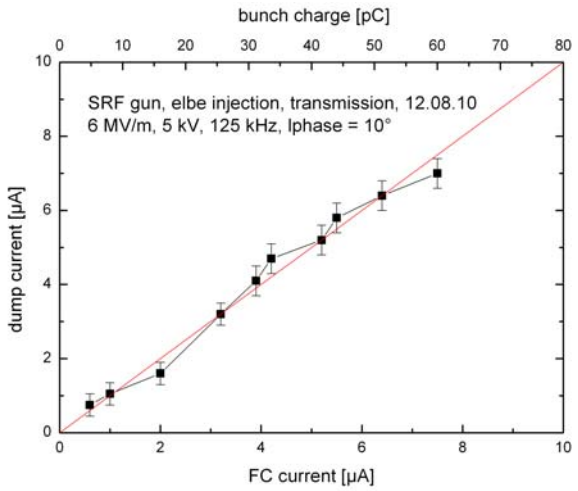

Figure 10. Transmission measurement of the SRF gun injection experiment. The diagram compares the current measured in the Faraday cup downstream the gun with the current measured in the beam dump ET1-CB.01after the switching magnet.

5. Summary

The SRF gun is now connected to the ELBE linear accelerator. The operation of the SRF gun as injector for ELBE has been demonstrated. The Cs_2Te photocathodes used in the gun showed sufficient quantum efficiency and long lifetime. Up to now, we did not found any cavity degradation, which may occur due to the operation of a normal conducting photocathode in the superconducting cavity. The handicap of the gun is the low acceleration gradient of 6 MV/m obtained with the present cavity. It has a strong influence on the beam parameters. Nevertheless, the gun is able to provide beam for ELBE and will be tested for user operation. In order to overcome the low-gradient problem, a new large grain 3½ cell niobium cavity with optimized shape has been designed, fabricated and will be tested soon.

Acknowledgements

We acknowledge the support of the European Community-Research Infrastructure Activity under the FP7 programme (EuCARD, contract number 227579), as well as the support of the German Federal Ministry of Education and Research grant 05 ES4BR1/8.

References

[1] Arnold A, Büttig H, Janssen D, Lehnert U, Michel P, Möller K, Murcek P, Schneider Ch, Schurig R, Staufenbiel F, Teichert J, Xiang R, Kamps T, Lipka D, Marhauser F, Lehmann W D, Stephan J, Volkov V, Will I and Klemz G 2007 *Nucl. Instr.and Meth. A* **577** 440

[2] Michel P, Büttig H, Gabriel F, Helm M, Lehnert U, Schneider Ch, Schurig R, Seidel W, Stehr D, Teichert J, Winnerl S and Wünsch R 2006 *Proc. International Free Electron Laser Conference FEL´06 (Berlin, Germany, 27 August - 01 September 2006)* pp 488-491

[3] Kamps T, Arnold A, Boehlick D, Dirsat M, Klemz G, Lipka D, Quast T, Rudolph J, Schenk M, Staufenbiel F, Teichert J and Will I 2008 *Review of Scientific Instruments* **79**, 093301

[4] Will I, Klemz G, Staufenbiel F and Teichert J 2006 *Proc. International Free Electron Laser Conference FEL´06 (Berlin, Germany, 27 August - 01 September 2006)* pp 564-566

[5] Teichert J, Arnold A, Büttig H, Janssen D, Justus M, Lehnert U, Michel P, Murcek P, Schamlott A, Schneider Ch, Schurig R, Staufenbiel F, Xiang R, Kamps T, Rudolph J, Schenk M, Klemz G and Will I 2008 *Proc. International Free Electron Laser Conference FEL´08 (Gyeongju, Korea, 24-29 August 2008)* pp. 467-472
[6] Xiang R, Arnold A, Buettig H, Janssen D, Justus M, Lehnert U, Michel P, Murcek P, Schamlott A, Schneider Ch, Schurig R, Staufenbiel F and Teichert J 2010 *Phys. Rev. ST Accel. Beams* **13** 043501
[7] K. Floettmann 1997 *TESLA-FEL report 1997-01, DESY*
[8] Powell R A, Spicer W E, Fisher G B and Gregory P 1973 *Physical Review B* **8** 3978
[9] Burrill A, Ben-Zvi I, Cole M, Rathke J, Kneisel P, Manus R and Rimmer R 2007 *Proceedings of PAC07 (Albuquerque, USA, 25-29 June 2007)* pp. 2544-2546
[10] Abe T, Kageyama T, Sakai H, Takeuchi Y and Yoshino K 2010 *Phys Rev. ST Accel Beams* **13** 102001